25th ABCM International Congress of Mechanical Engineering
October 20-25, 2019, Uberlândia, MG, Brazil

COB-2019-2415
MULTI-OBJECTIVE OPTIMIZATION OF THE MODAL CHARACTERISTICS OF TOW-STEERED CFRP PLATES

Daniel A. Pereira[1,2]
Thiago de P. Sales[1]
danielpe@ipt.br
tpsales@ita.br
Domingos A. Rade[1]
rade@ita.br

[1] ITA - Aeronautics Institute of Technology, Division of Mechanical Engineering, São José dos Campos, Brazil
[2] IPT - Institute for Technological Research, Lightweight Structures Laboratory, São José dos Campos, Brazil

Abstract. *In recent years, automatic fiber placement (AFP) machines have allowed the realization of variable stiffness composite laminates. Among these, tow-steered composites have been considered very promising. The problem of finding the optimal lamination sequence (lay-up) to maximize a specific design requirement is usually solved with design optimization. It is known that carbon-fiber reinforced polymers (CFRP) can be designed in order to improve damping characteristics by properly tuning geometric features such as fiber orientation. Therefore, the objective of this paper is to present a multi-objective optimization of CFRP tow-steered plates, aiming at maximizing modal frequencies and damping factors. Fiber trajectories are taken as design variables, as one tries to explore the benefits brought up by the steering technique. The dynamic model is derived by using a semi-analytical approach based on the combination of the Classical Lamination Theory with the Rayleigh-Ritz approach. The modal damping factors are calculated using the Strain Energy Method, which is based on the ratio between the stored and the dissipated energies, giving the specific damping capacity (SDC) for each vibration mode. Finally, the multi-objective optimization problem is solved using a variant of the NSGA-II algorithm. Results show that the tow-steered plates are the best choice for maximizing the modal damping and frequency characteristics of the considered plates for different boundary conditions.*

Keywords: *Composites, tow-steering, strain energy method, damping, multi-objective optimization*

1. INTRODUCTION

It is known that the increasing requirement on dynamic properties of lightweight structures will promote the development of high energy dissipation and high stiffness materials (Tang and Yan, 2018). In this context, it is widely recognized that composite materials, especially fiber-reinforced ones, have enormous potential for applications to lightweight structures. One of the main advantages of these materials is the possibility of being designed to comply with specific performance criteria by changing the relative fiber orientations of the plies. In addition, the current emergence of novel manufacturing techniques, such as automatic fiber placement (AFP), opens new possibilities for further improvement of composite structural components. In particular, it is currently possible to manufacture the so-called variable stiffness composite laminates (VSCL), which encompass those made with variable fiber spacing (VFSL) and those in which the fibers are deposited following curvilinear paths. The latter are known as tow-steered composites laminates (TSCL) (Ribeiro *et al.*, 2014). As compared to traditional composite laminates, VSCL provide the designer with a broader range of options to design composite plates considering multiple design goals, while minimizing weight penalties (Wu *et al.*, 2013). Under these motivations, various researchers have been investigating the vibrational (Abdalla *et al.*, 2007; Akhavan and Ribeiro, 2011; Guimarães *et al.*, 2017), aeroelastic (Stanford *et al.*, 2014; Guimaraes *et al.*, 2017) and buckling behavior (Wu *et al.*, 2012b, 2013) of tow-steered laminates.

Many researchers have proposed the tow-steering technique to increase the natural frequencies of composites; however, to the best knowledge of these authors, studies on the damping characteristics of TSCL, which is addressed here, had not been reported in the literature before. In terms of vibration behavior, damping of composite materials can be several orders of magnitude higher than that of traditional engineering materials, making them appealing for use in components undergoing dynamic loading (Treviso *et al.*, 2015). To study the effect of fiber orientation of constant stiffness laminates on the modal damping of composites, specific damping capacity (SDC) based strategies have proven adequate (Maheri and Adams, 2003; Maheri, 2011). Various authors have investigated the influence of layup on the damping levels of tra-

ditional composite plates (Hwang *et al.*, 1992; Berthelot, 2006; Abbaslou and Maheri, 2016). Wen-kai *et al.* (2016) have shown that the VSCL can be an efficient strategy to increase the damping performance of composites, while conducting damping optimization of a VSCL plate using the modal dissipative energy principle. Their results show that the damping properties of the VSCL plate can be increased by 50%–70%. However, in their approach, the VSCL are not modeled considering continuous fibers, therefore leading to optimized plates which should not be involved to manufacture. To alleviate on this issue, the tow-steering technique can be adopted as a suitable replacement, due to the well established manufacturing process through AFP, for example.

Based on the hypotheses of Kirchhoff plate theory, a dynamic model is formulated by associating the Classical Lamination Theory with the Rayleigh-Ritz approach. The modeling approach duly accounts for the curvilinear trajectory of the fibers on each lamina. The modal damping factors are calculated using the Strain Energy Method, which is based on the ratio between the stored and the dissipated energies. The values of natural frequencies and modal damping factors are then evaluated for different fiber trajectories in a multi-objective optimization framework. The multi-objective optimization problem is solved using a variant of the Fast Non-dominated Sorting Genetic Algorithm (NSGA-II). Most multi-objective GA do not require the user to prioritize, scale, or weigh objectives. Therefore, GA have been the most popular heuristic approach to multi-objective design and optimization problems (Konak *et al.*, 2006). Laminated composite plates are usually designed to maximize the fundamental frequency to avoid resonance in aerospace and naval structures. By considering tow-steered composite plates, it is possible to find better solutions for multi-objective problems. Therefore, the objective of this paper is to assess the use of tow-steering to maximize both fundamental modal frequency and damping factors of a quasi-isotropic plate, which is taken as a baseline, while considering free-free, simply supported, and fully clamped boundary conditions.

2. NUMERICAL MODELING

Among all the methodologies available for dealing with variable stiffness composite laminates, the tow-steering technique, in which the fiber angle scattering is used to produce curvilinear tow-paths over the layer, gives significant freedom for stiffness and damping tailoring in structural design. In the works of Wu *et al.* (2012b, 2013), the nonlinear variation of fiber angles changes over the plate according to Lagrange's interpolation polynomials, which are used to define the optimal design of the laminates, generating a family of fiber paths with different polynomial degrees, allowing high flexibility for optimization. In this definition, a set of $M \times N$ control points (Figure 1) are selected over the domain of the plate, each of which is associated with a value of fiber angle $\theta(x, y)$, which can be interpolated using:

$$\theta(x,y) = \sum_{m=0}^{M-1}\sum_{n=0}^{N-1} T_{mn} \cdot \prod_{m\neq i} \frac{x - x_i}{x_m - x_i} \cdot \prod_{n\neq j} \frac{y - y_j}{y_n - y_j}, \tag{1}$$

where T_{mn} are the control angles in the reference points (x_m, y_n). the constraints due to automated fiber placement machines for manufacturing curvilinear paths, many authors (Gurdal and Olmedo, 1993; Gürdal *et al.*, 2008) used processing techniques that result in fiber patterns that are parallel to one another; in such formulation, the fiber orientation is made to vary only along one of the coordinates. If the fiber angle is only allowed to vary along an axis, for example the x–axis,

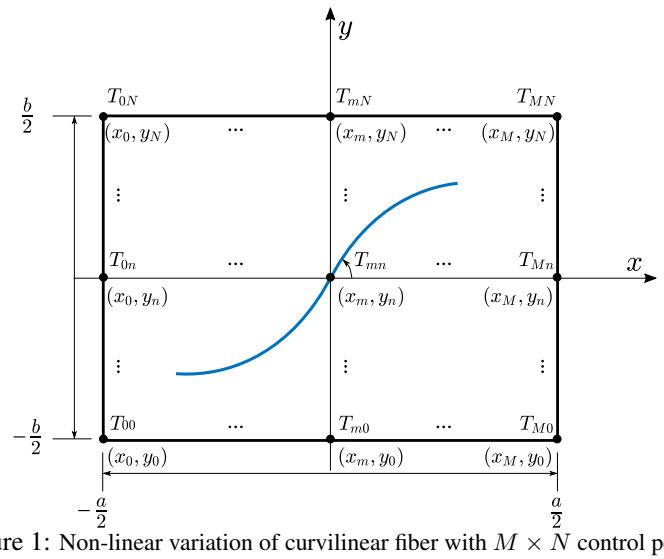

Figure 1: Non-linear variation of curvilinear fiber with $M \times N$ control points.

Eq. (1) simplifies to

$$\theta(x) = \sum_{m=0}^{M-1} T_m . \prod_{m \neq i} \frac{x - x_i}{x_m - x_i}. \tag{2}$$

Figure 2 shows the first three families of fiber paths, with straight fibers, linear and parabolic variation of Lagrange's polynomials, respectively. High-order paths cannot be properly manufactured because of defects that get introduced in the final part. The paths in y–axis are obtained by shifting the fibers along its direction (Waldhart, 1996).

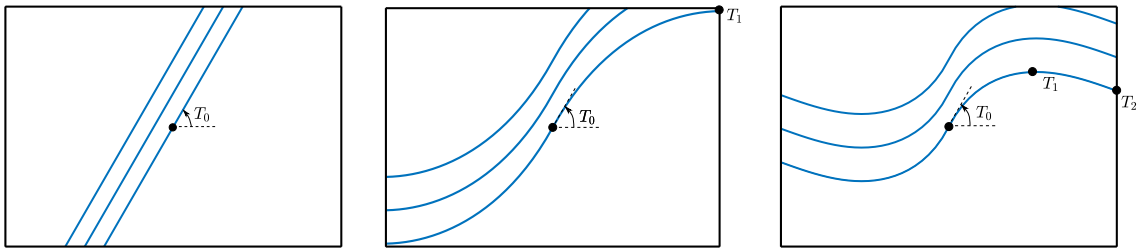

(a) Straight fibers (b) Linear variation (c) Parabolic variation

Figure 2: First three families of fiber paths generated by Lagrange's polynomials.

Equation (2) can be particularized to provide the expressions which consider constant, linear and parabolic distributions for the fiber angle interpolation function:

$$\theta(x) = T_0 \,, \tag{3}$$

$$\theta(x) = \tfrac{2}{a}(T_1 - T_0)|x| + T_0 \,, \tag{4}$$

$$\theta(x) = T_0 \left(\tfrac{2|x|}{a} - 1\right)\left(\tfrac{4|x|}{a} - 1\right) - 4T_1 \tfrac{2|x|}{a}\left(\tfrac{2|x|}{a} - 1\right) + T_2 \tfrac{2|x|}{a}\left(\tfrac{4|x|}{a} - 1\right) \,, \tag{5}$$

where a is the plate length along the x direction. In Eq. (4), T_0 and T_1 are the values of the fiber angle at $x = 0$ and at $x = a/2$. In Eq. (5), T_0, T_1 and T_2 denote the values of the fiber angles at positions $x = 0$, $x = a/4$ and $x = a/2$, respectively. In this work, the linear interpolation strategy (Eq. (4)) is chosen to conduct optimization, which is the simplest tow-steering configuration.

The procedure used for modeling damping follows the approach proposed by Adams and Bacon (1973), which is based on the assumption that the dissipated energy is associated to principal stress components at the ply level. For a given displacement field, the specific damping capacity (SDC, denoted by Ψ) is defined as the ratio of the dissipated strain energy per cycle of vibration (ΔU) to the maximum strain energy (U), i.e.:

$$\Psi = \Delta U / U \,. \tag{6}$$

When U and ΔU are computed for the displacement fields corresponding to a set of natural vibration modes, the SDC provides the modal damping factors associated to those modes. Hence, U and ΔU are formulated herein for the tow-steered laminates based on the developments presented by Maheri and Adams (2003).

According to the Rayleigh-Ritz method, the transverse displacement field of the plate $w(x, y, t)$ is approximated as:

$$w(x, y, t) = \sum_{m=0}^{M} \sum_{n=0}^{N} X_m(x) Y_n(y) q_{mn}(t). \tag{7}$$

The functions $X_m(x)$ and $Y_n(y)$ must be differentiable at least to the maximum order of the derivatives that appear in the expressions of the strain energy, and must obey at least the geometric boundary conditions of the problem. Here, these functions have been chosen as Legendre polynomials, which present superior convergence properties when capturing localized features (Wu *et al.*, 2012a,b). Equation (7) is therefore rewritten in terms of dimensionless coordinates ($\zeta = 2x/a$ and $\eta = 2y/b$) as follows:

$$w(\zeta, \eta, t) = (1+\zeta)^{c_1}(1-\zeta)^{c_2}(1+\eta)^{c_3}(1-\eta)^{c_4} \sum_{m=0}^{M} \sum_{n=0}^{N} X_m(\zeta) Y_n(\eta) q_{mn}(t), \tag{8}$$

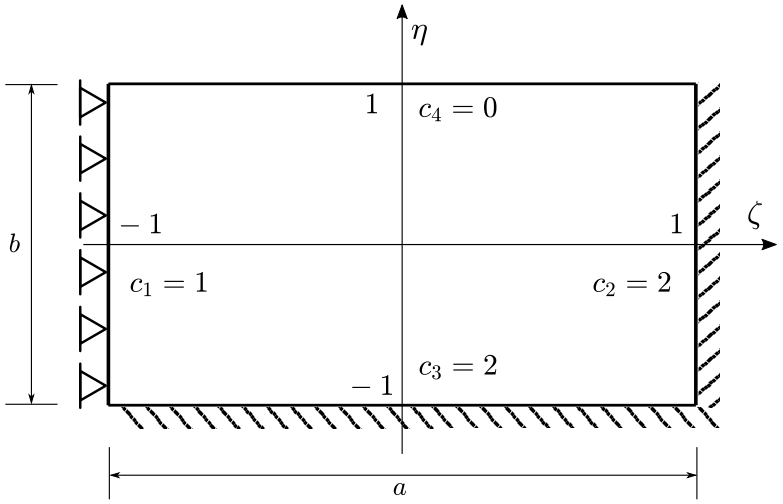

Figure 3: Parameters used to account for different boundary conditions in Eq. (8).

where:

$$X_m(\zeta) = \frac{1}{2^m}\sum_{k=0}^{m}\left(\begin{array}{c} m \\ k \end{array}\right)^2 (\zeta-1)^{m-k}(\zeta+1)^k,$$
$$Y_n(\eta) = \frac{1}{2^n}\sum_{k=0}^{n}\left(\begin{array}{c} n \\ k \end{array}\right)^2 (\eta-1)^{n-k}(\eta+1)^k. \tag{9}$$

It should be noticed that the parameters c_1 and c_2 enable one to account for different boundary conditions for the edges which obeys $x = \pm a/2$; whereas, c_3 and c_4 do the same, but for the edges satisfying $y = \pm b/2$. The free, simply-supported and clamped boundary conditions correspond to $c_i = 0, 1, 2$, respectively (Figure 3). Equation (8) can be written in a compact form as:

$$w(\zeta, \eta, t) = \mathbf{\Phi}(\zeta, \eta)\mathbf{q}(t), \tag{10}$$

in which $\mathbf{q}$ is a column vector collecting the generalized coordinates, and $\mathbf{\Phi}$ is a row vector of admissible functions.

Considering the absence of external forces, the equations of motion can be found as:

$$\mathbf{M}\,\ddot{\mathbf{q}}(t) + \mathbf{K}\,\mathbf{q}(t) = \mathbf{0}\,, \tag{11}$$

where $\mathbf{M}$ and $\mathbf{K}$ are the mass and stiffness matrices, given by:

$$\mathbf{M} = h\rho\frac{ab}{4}\int_{-1}^{1}\int_{-1}^{1}\mathbf{\Phi}^{\mathrm{T}}\mathbf{\Phi}\;d\zeta\,d\eta\,; \tag{12}$$

$$\mathbf{K} = \frac{ab}{4}\int_{-1}^{1}\int_{-1}^{1}\left\{D_{11}\frac{\partial^2\mathbf{\Phi}}{\partial x^2}^{\mathrm{T}}\frac{\partial^2\mathbf{\Phi}}{\partial x^2} + 2D_{12}\frac{\partial^2\mathbf{\Phi}}{\partial x^2}^{\mathrm{T}}\frac{\partial^2\mathbf{\Phi}}{\partial y^2} + D_{22}\frac{\partial^2\mathbf{\Phi}}{\partial y^2}^{\mathrm{T}}\frac{\partial^2\mathbf{\Phi}}{\partial y^2}\right.$$
$$\left. + 4D_{16}\frac{\partial^2\mathbf{\Phi}}{\partial x^2}^{\mathrm{T}}\frac{\partial^2\mathbf{\Phi}}{\partial x\partial y} + 4D_{26}\frac{\partial^2\mathbf{\Phi}}{\partial y^2}^{\mathrm{T}}\frac{\partial^2\mathbf{\Phi}}{\partial x\partial y} + 4D_{66}\frac{\partial^2\mathbf{\Phi}}{\partial x\partial y}^{\mathrm{T}}\frac{\partial^2\mathbf{\Phi}}{\partial x\partial y}\right\}d\zeta\,d\eta\,. \tag{13}$$

In these, h is the plate thickness; b is the plate length along y; ρ denotes the material density; and D_{ij} are rigidity coefficients, which incorporate the contributions from the plies of the laminate, as well as the tow-steering strategy used for the fibers' paths, being computed from:

$$\mathbf{D}_{ij} = \sum_{k=1}^{N}\left(\int_{z_{k-1}}^{z_k}\bar{\mathbf{Q}}_k z^2 dz\right) = \sum_{k=1}^{N}\int_{z_{k-1}}^{z_k}\left[\begin{array}{ccc}\bar{Q}_{11} & \bar{Q}_{12} & \bar{Q}_{16}\\ \bar{Q}_{12} & \bar{Q}_{22} & \bar{Q}_{26}\\ \bar{Q}_{16} & \bar{Q}_{26} & \bar{Q}_{66}\end{array}\right]_k z^2 dz = \frac{1}{3}\sum_{k=1}^{N}(z_k^3 - z_{k-1}^3)\bar{\mathbf{Q}}_k, \tag{14}$$

with z_{k-1} and z_k being the lower and upper thickness limits of each layer (k) and $\bar{\mathbf{Q}}_k = \mathbf{T}_k^{\mathrm{T}}\mathbf{Q}_k\mathbf{T}_k$. The 'stiffness' matrix $\mathbf{Q}_k$ is given by:

$$\mathbf{Q}_k = \left[\begin{array}{ccc} Q_{11} & Q_{12} & 0\\ Q_{12} & Q_{22} & 0\\ 0 & 0 & Q_{66}\end{array}\right] \tag{15}$$

where:

$$Q_{11} = \frac{E_1}{1-\nu_{12}\nu_{21}}, \quad Q_{22} = \frac{E_2}{1-\nu_{12}\nu_{21}}, \quad Q_{12} = Q_{21} = \frac{\nu_{12}E_2}{1-\nu_{12}\nu_{21}}, \quad Q_{66} = G_{12}, \tag{16}$$

and $\mathbf{T}_k$ is the transformation matrix of the strain vector from the global coordinate system $(x-y)$ to the principal coordinates reference frame $(1-2)$, which is given by:

$$\mathbf{T}_k = \begin{bmatrix} c^2 & s^2 & cs \\ s^2 & c^2 & -cs \\ -2cs & 2cs & c^2-s^2 \end{bmatrix}^{(k)}, \tag{17}$$

where $c = \cos\theta^{(k)}$ and $s = \sin\theta^{(k)}$. For tow-steered composite laminates, $\theta^{(k)}$ is function of x, and therefore $\mathbf{T}_k(\theta^{(k)}(x))$ (cf. Eq. (4)).

From Eq. (11), the following eigenvalue problem can be established:

$$\left(\mathbf{K} - \omega_j^2\,\mathbf{M}\right)\boldsymbol{\delta}_j = 0\,, \tag{18}$$

from which natural frequencies ω_j and the corresponding modal shapes $\boldsymbol{\delta}_j$ may be obtained.

To determine the SDC using Eq. (6), the modal strain and the modal dissipated strain energies are also required:

$$U_j = \tfrac{1}{2}\,\boldsymbol{\delta}_j^{\mathrm{T}}\,\mathbf{K}\,\boldsymbol{\delta}_j\,, \quad \Delta U_j = \tfrac{1}{2}\,\boldsymbol{\delta}_j^{\mathrm{T}}\,\mathbf{K_d}\,\boldsymbol{\delta}_j\,, \tag{19}$$

where:

$$\mathbf{K_d} = \frac{ab}{4}\int_{-1}^{1}\int_{-1}^{1}\left\{ d_{11}\frac{\partial^2\boldsymbol{\Phi}}{\partial x^2}^{\mathrm{T}}\frac{\partial^2\boldsymbol{\Phi}}{\partial x^2} + (d_{12}+d_{21})\frac{\partial^2\boldsymbol{\Phi}}{\partial x^2}^{\mathrm{T}}\frac{\partial^2\boldsymbol{\Phi}}{\partial y^2} + d_{22}\frac{\partial^2\boldsymbol{\Phi}}{\partial y^2}^{\mathrm{T}}\frac{\partial^2\boldsymbol{\Phi}}{\partial y^2} \right.$$
$$\left. +2(d_{16}+d_{61})\frac{\partial^2\boldsymbol{\Phi}}{\partial x^2}^{\mathrm{T}}\frac{\partial^2\boldsymbol{\Phi}}{\partial x\partial y} + 2(d_{26}+d_{62})\frac{\partial^2\boldsymbol{\Phi}}{\partial y^2}^{\mathrm{T}}\frac{\partial^2\boldsymbol{\Phi}}{\partial x\partial y} + 4d_{66}\frac{\partial^2\boldsymbol{\Phi}}{\partial x\partial y}^{\mathrm{T}}\frac{\partial^2\boldsymbol{\Phi}}{\partial x\partial y}\right\} d\zeta\, d\eta\,, \tag{20}$$

in which d_{ij} are defined in a similar way to D_{ij}, but taking into account the so-called "damped stiffness matrix". It relies on the availability of damping properties of the material, namely ψ_L, ψ_T and ψ_{LT} (Maheri and Adams, 2003), which are the longitudinal, transverse and longitudinal–shear specific damping capacities of an unidirectional lamina. One has that:

$$\mathbf{d}_{ij} = \sum_{k=1}^{N}\left(\int_{z_{k-1}}^{z_k}\mathbf{R}_k z^2 dz\right) = \sum_{k=1}^{N}\int_{z_{k-1}}^{z_k}\begin{bmatrix} R_{11} & R_{12} & R_{16} \\ R_{21} & R_{22} & R_{26} \\ R_{61} & R_{62} & R_{66} \end{bmatrix}_k z^2 dz = \frac{1}{3}\sum_{k=1}^{N}(z_k^3 - z_{k-1}^3)\mathbf{R}_k \tag{21}$$

in which $\mathbf{R}_k$ is given by $\mathbf{R}_k = \mathbf{T}_k^{\mathrm{T}}\boldsymbol{\psi}_k\mathbf{Q}_k\mathbf{T}_k$ and:

$$\boldsymbol{\psi}_k = \begin{bmatrix} \psi_L & 0 & 0 \\ 0 & \psi_T & 0 \\ 0 & 0 & \psi_{LT} \end{bmatrix}. \tag{22}$$

These contributions are associated to the deflection of the fiber ψ_L (smallest SDC), related to the stress distribution in a direction perpendicular to the reinforced fiber axis ψ_T, and to the in-plane shear stress ψ_{LT}, which are nearly exclusively determined by the matrix (Tang and Yan, 2018), having hence relatively high SDCs. It is relevant to highlight that the modal damping is a weighted average between the longitudinal, transverse and longitudinal–shear effects of the material damping.

According to Zabaras and Pervez (1990), the relation between the specific damping capacity and the damping ratio of the laminate for the j-th mode is given by:

$$\zeta_j = \frac{\Psi_j}{4\pi} = \frac{1}{4\pi}\frac{\boldsymbol{\delta}_j^{\mathrm{T}}\,\mathbf{K_d}\,\boldsymbol{\delta}_j}{\boldsymbol{\delta}_j^{\mathrm{T}}\,\mathbf{K}\,\boldsymbol{\delta}_j} \tag{23}$$

3. RESULTS

Table 1 shows the values of the first six natural frequencies and SDCs obtained from the Rayleigh-Ritz (R-R) model, considering 81 generalized coordinates ($M = N = 8$), which are compared to the experimental results from Maheri and Adams (2003) for the free-free boundary conditions. The plate is made of eight plies, using the material 913C-HTA. The

lay-up is [0°,90°,45°,-45°]$_s$ resulting in a quasi-isotropic laminate, with $a = 287$ mm, $b = 287$ mm, $h = 1.045$ mm. Also illustrated are the mode shapes corresponding to the six vibration modes considered. Tables 2 and 3 present analogous results, but considering different boundary conditions: simply-supported and fully-clamped, respectively.

For quasi-isotropic composite panels, the in-plane mechanical properties do not vary with direction, as exemplified by plates with ply configuration equal to 0°, 45° and 90°. For most cases, the quasi-isotropic configuration is an inefficient use of the composite material. However, these arrangements are still used in many aircraft structures (Dutton *et al.*, 2004). One can maximize the frequency and damping of the quasi-isotropic composite by changing the fiber orientation through the layers, and also the lay-up orientation of each layer. Optimization is therefore carried out by considering: i) conventional plates with straight fibers (Fig. 2(a)), here denoted as non-steered plates (NS), and ii) plates with variable stiffness layers, with linear variation for the fiber orientation (Fig. 2(b)), abbreviated as tow-steered plates (TS). Moreover, from Tables 1, 2 and 3, the frequency and damping for the fundamental mode of vibration are 33.4 Hz and 3.74% for the free-free boundary condition, 62.4 Hz and 1.57% for simply-supported, and 126.7 Hz and 1.18% for fully-clamped. This goes to show how significant the boundary conditions are to the vibration characteristics of structures. Since BCs are imperfect in reality, and also appear in mixed combinations, their influence is also assessed.

Table 1: Comparison between the Rayleigh-Ritz simulation results for a quasi-isotropic laminate [0°, 90°, 45°,-45°]$_s$ with $a = 287$ mm, $b = 287$ mm, $h = 1.045$ mm and material 913C-HTA.

Mode shapes		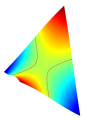	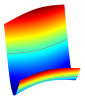	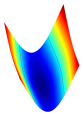	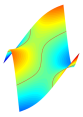		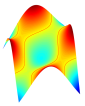
Freq. (Hz)	**R-R**	**33.4**	**72.8**	**95.0**	**98.3**	**117.0**	**180.8**
	Exp.[2]	38.5	71.4	94.5	101.5	120.2	180.9
SDC (%)	**R-R**	**3.74**	**1.20**	**0.81**	**2.41**	**1.74**	**2.50**
	Exp.[2]	3.18	1.42	0.91	2.66	1.93	2.80

913C-HTA: $E_1 = 124.5$ GPa, $E_2 = 10.2$ GPa, $G_{12} = 6.3$ GPa, ν_{12}=0.34, $\psi_L = 0.55\%$, $\psi_T = 4.98\%$, $\psi_{LT} = 5.92\%$, $\rho = 1532$ kg/m^3
[2] Experimental results obtained from Table 4 of Maheri and Adams (2003).

Table 2: Rayleigh-Ritz simulation results for the quasi-isotropic laminate under study [0°, 90°, 45°,-45°]$_s$ with simply-supported boundary conditions (SSSS).

Mode shapes		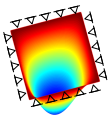	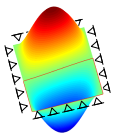	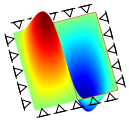	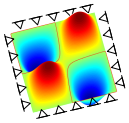	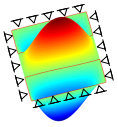	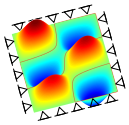
Freq. (Hz)	**R-R**	62.4	151.1	183.0	249.1	311.0	388.6
SDC (%)	**R-R**	1.57	1.56	1.11	1.59	1.41	1.66

Table 3: Rayleigh-Ritz simulation results for the quasi-isotropic laminate under study [0°, 90°, 45°,-45°]$_s$ with fully-clamped boundary conditions (CCCC).

Mode shapes		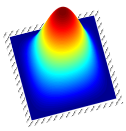	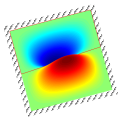	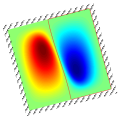	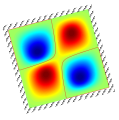	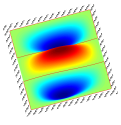	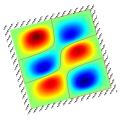
Freq. (Hz)	**R-R**	126.7	236.7	282.9	363.4	424.2	523.3
SDC (%)	**R-R**	1.18	1.37	1.00	1.35	1.33	1.48

3.1 Maximizing the Fundamental Frequency and Damping

Composite laminated plates are usually designed for maximum fundamental frequency constraints, and they are particularly attractive because the vibration response can be optimized by tailoring the fiber angles of different layers without incurring weight penalties (Abdalla *et al.*, 2007). New configurations of composite plates can be envisioned to meet also specific performance criteria on damping by changing the relative fiber orientations of the plies. It is known that the main

reason behind the higher damping capacity of the FRP composites, compared to metals, is the viscoelastic behavior of the polymeric matrix (Treviso *et al.*, 2015; Chandra *et al.*, 1999). Figure 4 shows a comparison between two Pareto fronts constructed by requiring simultaneous maximization of the fundamental frequency and the corresponding SDC, considering constant stiffness composite plates (labeled non-steered - NS); and variable stiffness composite configurations, based on the tow-steering technique (labeled tow-steered - TS). For both types of plates, the material was considered to be 913C-HTA. Design variables were selected as the fiber orientation in each ply, for the non-steered plates; and as the angles T_0 and T_1 for each ply in the tow-steered plates. Figures 4(a), (b) and (c) show, respectively, the optimum designs for the CFRP plates, as functions of their fundamental natural frequency and SDC, for the completely free, simply-supported and fully-clamped boundary conditions, respectively.

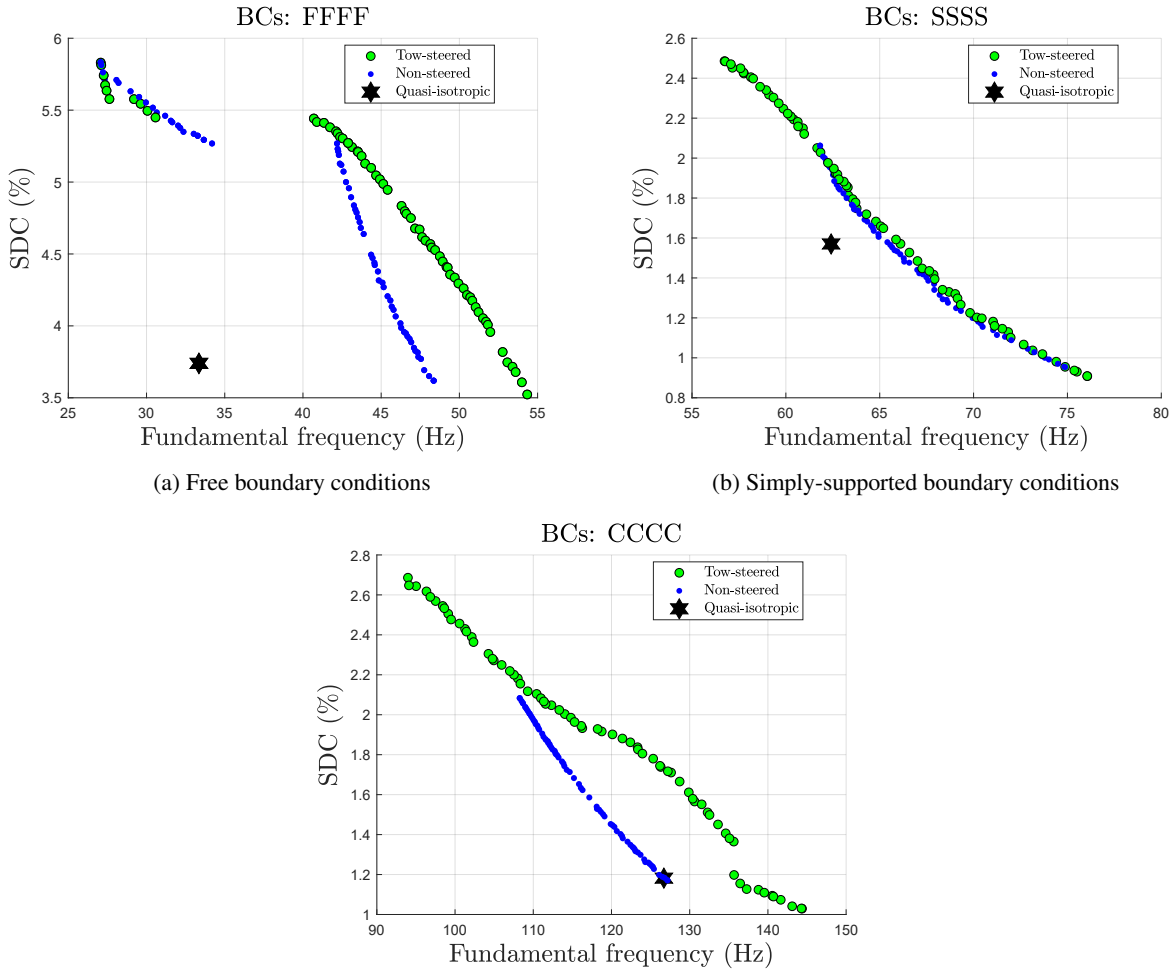

(a) Free boundary conditions

(b) Simply-supported boundary conditions

(c) Fully-clamped boundary conditions

Figure 4: Pareto fronts of the non-steered and tow-steered composite plates obtained from a multi-objective optimization set to maximize the fundamental frequency and damping of symmetric laminates containing eight plies.

In Fig. 4, each marker represents a plate configuration with eight layers. From Fig. 4(a) one can see that both tow-steered (green circles) and non-steered (blue dots) plates can increase significantly the frequency and damping of the quasi-isotropic plate (presented in the graph as a black hexagram). One also can conclude that the tow-steered laminates can provide significant improvements in terms of frequency and damping, as compared to the non-steered plates, after 42.3 Hz, approximately, in which the gap between the two Pareto fronts increases. At 48.36 Hz, which is the maximum frequency achieved by the non-steered plate, the corresponding optimal tow-steered plate presents a specific damping capacity equal to 4.54%, which is 25% higher than the non-steered plate (3.62%). It is also possible to conclude that, for lower frequencies, the optimal tow-steered plates are close to the optimal non-steered ones. From Fig. 4(b), which shows the Pareto fronts for the plates under simply-supported boundary conditions, there is no gap between the TS and NS plates. However, the TS plates enable values of SDC which are greater than 2.05%, which is the maximum SDC achievable by the NS plates. The frequency does not present significant improvement, and the quasi-isotropic laminate is close to the Pareto fronts. Finally, from Fig. 4(c) the quasi-isotropic plate is on top of the Pareto front of the non-steered plates, in which the NS plates are not able to increase the fundamental frequency. The optimal tow-steered plates, in contrast,

with fully-clamped boundary conditions, presents significant improvements over the entire NS Pareto front, allowing for increased frequency and improved SDC simultaneously. For the fundamental frequency equal to 126.7 Hz, which is the largest achieved by a NS plate, the tow-steered plate gives a SDC equal to 1.72%, which is 46% greater than the SDC value associated with the NS plate and the baseline quasi-isotropic plate (SDC equal to 1.18%). It is essential to highlight that almost all real panels used in practice are neither free–free nor simply-supported (Maheri, 2011). Instead, practical panels usually have a combination of clamped, free, and hinged boundary conditions, and therefore, the tow-steering technique can lead to better multi-objective solution for the design requirements.

Table 4 presents the maximum fundamental frequency and SDC for the tow-steered and non-steered plates and their lay-up configurations concerning each set of boundary conditions. It is important to realize that a non-steered ply can be obtained when T_0 is made equal to T_1. The laminates of Plates 1 and 3 present layers with similar configurations, approximately [0°, 0°, 0°,0°]$_s$, showing that for maximizing the damping of a plate subjected to FFFF boundary conditions, non-steered arrangements can be more efficient. The reason for this observation is that the first mode of vibration, for these BCs, presents pure twist-type deformations, and the SDC 5.83% is close to the largest material damping property, ψ_{LT} = 5.92%, which happen when the polymer material of the matrix experiences intense shear, and the SDC value tends to the longitudinal shear material damping property ψ_{LT}. The scenario changes when one takes a look at the tow-steered Plates 5 and 9, which have been optimized considering the SSSS and CCCC boundary conditions, respectively. Now, the variable stiffness strategy is able to increase the effect of energy dissipation within the matrix over the plate, and also through the layers, and the damping becomes greater than the one provided by the non-steered Plates 7 and 11. One also finds that non-steered Plates 7 and 11 have their layers with orientation close to 45°, which is essential to enhance the shear deformation mode in the matrix increasing the percentage contribution of the longitudinal shear material damping ψ_{LT} to the modal SDC. It is evident from Table 4 that the variable stiffness composite plates can increase the maximum fundamental frequency more than the non-steered plates for all considered boundary conditions. Figures 5, 6 and 7 shows the lay-up configurations of the plates from Table 4, optimized for the FFFF (Plates 1 to 4), SSSS (Plates 5 to 8) and CCCC (Plates 9 to 12) boundary conditions.

Table 4: Fundamental natural frequency, SDC and lay-up of the plates highlighted in Fig. 4, following the terminology of $< T_0/T_1 >$ for tow-steered plates and θ for non-steered plies.

N°	Obj.	B.C.	Lay-up	Freq. (Hz)	SDC (%)	Layer 1	Layer 2	Layer 3	Layer 4
1	Max. SDC	FFFF	Tow	27.1	**5.83**	<1°/1°>	<2°/0°>	<1°/1°>	<0°/1°>
2	Max. Freq.	FFFF	Tow	**54.2**	3.54	<23°/77°>	<-40°/-60°>	<-36°/-37°>	<16°/-35°>
3	Max. SDC	FFFF	Non	27.1	**5.83**	θ =0°	θ =0°	θ =0°	θ =0°
4	Max. Freq.	FFFF	Non	**48.1**	3.66	θ =-43°	θ =46°	θ =5°	θ =0°
5	Max. SDC	SSSS	Tow	56.7	**2.49**	<67°/0°>	<64°/2°>	<49°/5°>	<36°/19°>
6	Max. Freq.	SSSS	Tow	**76.0**	0.91	<36°/49°>	<-45°/-41°>	<-46°/-45°>	<14°/12°>
7	Max. SDC	SSSS	Non	61.8	**2.06**	θ =43°	θ =42°	θ =43°	θ =44°
8	Max. Freq.	SSSS	Non	**74.9**	0.96	θ =38°	θ =-44°	θ =-24°	θ =8°
9	Max. SDC	CCCC	Tow	94.0	**2.69**	<68°/-66°>	<70°/-69°>	<71°/-61°>	<28°/-39°>
10	Max. Freq.	CCCC	Tow	**144.4**	1.03	<90°/-1°>	<-83°/0°>	<73°/3°>	<32°/-17°>
11	Max. SDC	CCCC	Non	108.3	**2.08**	θ =44°	θ =46°	θ =45°	θ =38°
12	Max. Freq.	CCCC	Non	**127.2**	1.17	θ =0°	θ =-90°	θ =0°	θ =0°

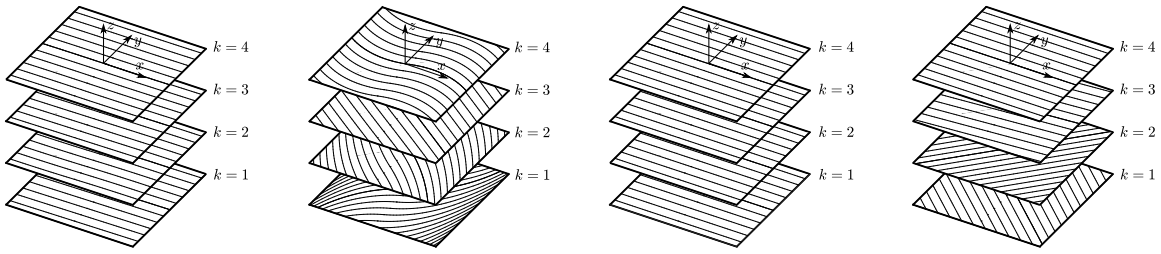

(a) Plate 1 (b) Plate 2 (c) Plate 3 (d) Plate 4

Figure 5: Lay-up of the CFRP Plates 1 to 4, optimized for the fully-free (FFFF) boundary conditions.

Figure 8 helps assess the results given in Table 4, ans shows the maximum frequency and SDC obtained from the Pareto fronts for non-steered and tow-steered plates for the three different boundary conditions that have been investigated. Figure 8(a) shows that the maximum gain in frequency is 62%, 22% and 14% for the FFFF, SSSS and CCCC boundary conditions, which are greater than those provided by the non-steered plates 44%, 20% and 0%, compared to the quasi-isotropic plate. One concludes that the variable stiffness strategy can be effective to increase the fundamental

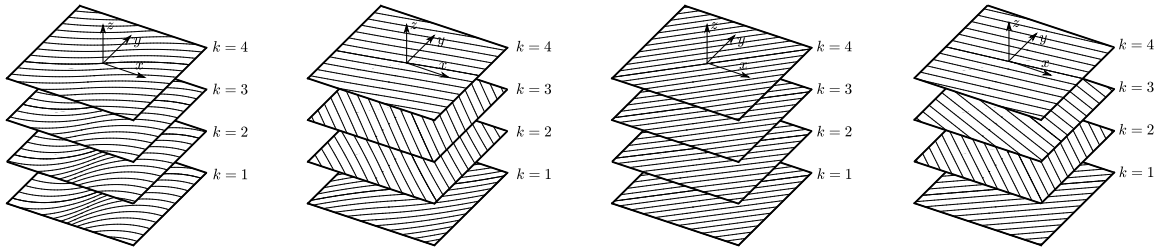

(a) Plate 5 (b) Plate 6 (c) Plate 7 (d) Plate 8

Figure 6: Lay-up of the CFRP Plates 5 to 8, optimized for the simply-supported (SSSS) boundary conditions.

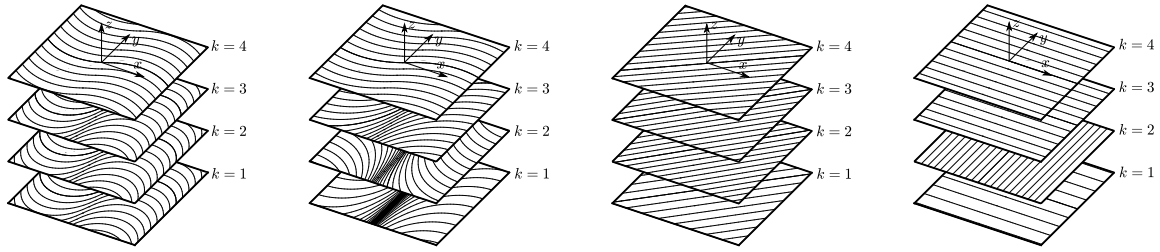

(a) Plate 9 (b) Plate 10 (c) Plate 11 (d) Plate 12

Figure 7: Lay-up of the CFRP Plates 9 to 12, optimized for the fully-clamped (CCCC) boundary conditions.

frequency of plates subject to FFFF boundary conditions. From Figure 8(b), the damping of the TS and NS plates show the same improvement of 83% for when boundary conditions are of the FFFF type. However, for the SSSS and CCCC boundary conditions the optimized tow-steered plates provide superior gains of 59% and 128% in specific damping capacity, respectively. In the fully-clamped, optimized TS plate, this happens because its fibers are able to increase the shear deformation within the polymer matrix, in the middle of the plate, which is essential since the vibration mode shape associated with the fundamental frequency presents the largest deformation at this location. It is important to remember that these results have been obtained for a linear variation of the curvilinear fibers, using Lagrange polynomials. If one increases the polynomial function order, we should observe an increased influence of the tow-steered technique on the frequency, which have been studied by Guimarães *et al.* (2017), as well as on damping. Nevertheless, trade-offs should be analyzed carefully, since the complexity of the fiber trajectory should impose problems on manufacturability of such plates (Falcó *et al.*, 2014).

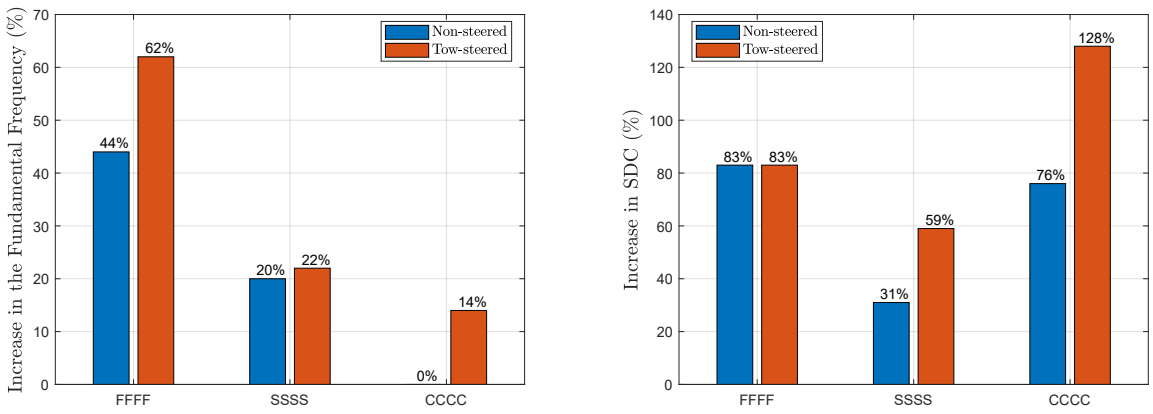

(a) Gain in frequency (b) Gain in SDC

Figure 8: Gains in (a) frequency and (b) damping in comparison with the quasi-isotropic laminate $[0, 90, 45, -45]_s$ for the first mode of vibration of plates subjected to FFFF, SSSS and CCCC boundary conditions (number inside each bar refers to designation used in Tables 1, 2 and 3).

4. CONCLUSION

In the present investigation, numerical multi-objective optimization was used to maximize the fundamental frequency and damping of a quasi-isotropic composite plate, which is an inefficient use of the composite material, for three different boundary condition sets. The tow-steered configurations have been defined by only two geometrical parameters, T_0 and T_1, for each layer of the laminate. From shown results, the tow-steering technique allowed for the best designs both in terms of frequency (which is increased by up to 62%, for the fully-free boundary condition), and damping (increased by 128% for the fully-clamped boundary condition). It should be possible to increase even more the effect of variable stiffness in a composite by increasing the order of the Lagrange polynomial approximation, but this would make the composite difficult to manufacture. The main contribution of this work is the confirmation that fiber steering can be an effective strategy for the design of composite laminates in terms of their dynamic behavior, allowing for tailoring of modal frequency and damping. In particular, it has been found that damping levels can be significantly increased by exploring fiber steering.

5. ACKNOWLEDGEMENTS

The authors acknowledge the National Council for Scientific and Technological Development (CNPq) (grants #301633/2013-3, #402238/2013-3 and #145439/2015-1), the National Institute of Science and Technology of Smart Structures in Engineering (INCT-EIE), FAPEMIG, Fundação de Apoio ao Instituto de Pesquisas Tecnológicas (FIPT) and São Paulo State Research Agency (FAPESP) grant #2015/20363-6 for the financial support to their research work.

6. REFERENCES

Abbaslou, A. and Maheri, M., 2016. "Prediction of the damping properties of fiber-reinforced polymer composite panels with arbitrary geometries". *Proceedings of the Institution of Mechanical Engineers, Part C: Journal of Mechanical Engineering Science*, Vol. 232, No. 2, pp. 275–283.

Abdalla, M.M., Setoodeh, S. and Gürdal, Z., 2007. "Design of variable stiffness composite panels for maximum fundamental frequency using lamination parameters". *Composite structures*, Vol. 81, No. 2, pp. 283–291.

Adams, R. and Bacon, D., 1973. "Effect of fibre orientation and laminate geometry on the dynamic properties of cfrp". *Journal of Composite Materials*, Vol. 7, No. 4, pp. 402–428.

Akhavan, H. and Ribeiro, P., 2011. "Natural modes of vibration of variable stiffness composite laminates with curvilinear fibers". *Composite Structures*, Vol. 93, No. 11, pp. 3040–3047.

Berthelot, J.M., 2006. "Damping analysis of laminated beams and plates using the ritz method". *Composite Structures*, Vol. 74, No. 2, pp. 186–201.

Chandra, R., Singh, S. and Gupta, K., 1999. "Damping studies in fiber-reinforced composites–a review". *Composite structures*, Vol. 46, No. 1, pp. 41–51.

Dutton, S., Kelly, D. and Baker, A., 2004. *Composite materials for aircraft structures*. American Institute of Aeronautics and Astronautics.

Falcó, O., Mayugo, J., Lopes, C., Gascons, N., Turon, A. and Costa, J., 2014. "Variable-stiffness composite panels: As-manufactured modeling and its influence on the failure behavior". *Composites Part B: Engineering*, Vol. 56, pp. 660–669.

Guimarães, T., Pereira, D. and Rade, D., 2017. "Dynamic behavior and optimization of tow steered composite plates". In *International Symposium on Dynamic Problems of Mechanics*. Springer, pp. 169–184.

Guimaraes, T.A., Castro, S.G., Rade, D.A. and Cesnik, C.E., 2017. "Panel flutter analysis and optimization of composite tow steered plates". In *58th AIAA/ASCE/AHS/ASC Structures, Structural Dynamics, and Materials Conference*. p. 1118.

Gürdal, Z., Tatting, B. and Wu, C., 2008. "Variable stiffness composite panels: Effects of stiffness variation on the in-plane and buckling response". *Composites Part A: Applied Science and Manufacturing*, Vol. 39, No. 5, pp. 911 – 922. ISSN 1359-835X. doi:http://dx.doi.org/10.1016/j.compositesa.2007.11.015. URL `http://www.sciencedirect.com/science/article/pii/S1359835X07002643`.

Gurdal, Z. and Olmedo, R., 1993. "In-plane response of laminates with spatially varying fiber orientations-variable stiffness concept". *AIAA journal*, Vol. 31, No. 4, pp. 751–758.

Hwang, S., Gibson, R. and Singh, J., 1992. "Decomposition of coupling effects on damping of laminated composites under flexural vibration". *Composites Science and Technology*, Vol. 43, No. 2, pp. 159–169.

Konak, A., Coit, D.W. and Smith, A.E., 2006. "Multi-objective optimization using genetic algorithms: A tutorial". *Reliability Engineering & System Safety*, Vol. 91, No. 9, pp. 992–1007.

Maheri, M.R. and Adams, R., 2003. "Modal vibration damping of anisotropic frp laminates using the rayleigh–ritz energy minimization scheme". *Journal of sound and vibration*, Vol. 259, No. 1, pp. 17–29.

Maheri, M., 2011. "The effect of layup and boundary conditions on the modal damping of frp composite panels". *Journal of Composite Materials*, Vol. 45, No. 13, pp. 1411–1422.

Ribeiro, P., Akhavan, H., Teter, A. and Warmiński, J., 2014. "A review on the mechanical behaviour of curvilinear fibre composite laminated panels". *Journal of Composite Materials*, Vol. 48, No. 22, pp. 2761–2777.

Stanford, B.K., Jutte, C.V. and Chauncey Wu, K., 2014. "Aeroelastic benefits of tow steering for composite plates". *Composite Structures*, Vol. 118, pp. 416–422. ISSN 0263-8223.

Tang, X. and Yan, X., 2018. "A review on the damping properties of fiber reinforced polymer composites". *Journal of Industrial Textiles*, p. 1–29.

Treviso, A., Van Genechten, B., Mundo, D. and Tournour, M., 2015. "Damping in composite materials: Properties and models". *Composites Part B: Engineering*, Vol. 78, pp. 144–152.

Waldhart, C., 1996. *Analysis of tow-placed, variable-stiffness laminates*. Ph.D. thesis, Virginia Tech.

Wen-kai, Q., Xian-tao, Y. and Cheng, S., 2016. "Research on damping properties optimization of variable-stiffness plate". In *Journal of Physics: Conference Series*. IOP Publishing, Vol. 744, p. 012114.

Wu, Z., Raju, G. and Weaver, P.M., 2012a. "Comparison of variational, differential quadrature, and approximate closed-form solution methods for buckling of highly flexurally anisotropic laminates". *Journal of Engineering Mechanics*, Vol. 139, No. 8, pp. 1073–1083.

Wu, Z., Weaver, P.M. and Raju, G., 2013. "Postbuckling optimisation of variable angle tow composite plates". *Composite Structures*, Vol. 103, pp. 34–42.

Wu, Z., Weaver, P.M., Raju, G. and Chul Kim, B., 2012b. "Buckling analysis and optimisation of variable angle tow composite plates". *Thin-Walled Structures*, Vol. 60, pp. 163–172.

Zabaras, N. and Pervez, T., 1990. "Viscous damping approximation of laminated anisotropic composite plates using the finite element method". *Computer methods in applied mechanics and engineering*, Vol. 81, No. 3, pp. 291–316.

7. RESPONSIBILITY NOTICE

The authors are the only responsible for the printed material included in this paper.